PERGAMON

International Journal of Heat and Mass Transfer 42 (1999) 2119–2127

International Journal of HEAT and MASS TRANSFER

Estimation of thermal contact resistance during the first stages of metal solidification process: I—experiment principle and modelisation

T. Loulou*, E.A. Artyukhin, J.P. Bardon

Laboratoire de Thermocinétique, I.S.I.T.E.M., La Chantrerie, BP 90604, F-44306, Nantes, France

Received 13 March 1997; in final form 18 September 1998

Abstract

This paper describes a simple experimental method for obtaining the thermal contact resistance between a metal casting and the mold. A specific model has been developed for the study of heat transfer across the metal–mold interface. This study uses a combination method of experimental and numerical procedures to obtain the thermal contact resistance during the first stages of the metal casting. Experimental work is performed to obtain measurable quantities such as thermal histories at various and selected thermocouple locations. The numerical work is performed to obtain temperature surface distribution and the inner gradient temperature by solving the inverse heat conduction problem in the mold region and by solving a direct heat phase change problem in the casting region.

Nomenclature

A constant
c constant coefficient
Cp heat capacity
d descent direction parameter
$\mathbf{D}$ vector of descent direction parameters
$f(t)$ measured temperature
H enthalpy
L latent heat
J residual functional
M number of parameter
N number of sensors, number of measurement points
P number of coefficient in smoothing
$\mathscr{R}(t)$ thermal contact resistance
t time
$T_c(x,t)$ casting temperature
$T_s(x,t)$ substrate temperature
u unknown parameter
$\mathbf{U}$ vector of unknown parameters
$U(t)$ unknown function
x space.

Greek symbols

α constant, thermal diffusivity
β parameter in descent direction
γ descent parameter
δ integrated measurement error
Δ small variation
$\Delta T(x,t)$ temperature variation
λ thermal conductivity
ρ density
σ standard deviation
φ heat flux, basis functions
$\psi(x,t)$ adjoint variable
∇ gradient
$\nabla \boldsymbol{J}$ vector of residual functional gradient.

Subscripts

c casting
int interface
f final
i ith position, ith time step
l liquid

* Corresponding author. E-mail; loulou@isitem.univ-nantes.fr

0017–9310/99/$ - see front matter
PII: S0017–9310(98)00333–0

m melting
s solid, substrate.

Superscripts
i number of layers, initial
s iteration number
T transpose.

1. Introduction

During metal casting the contact between the metal and the mold wall is not perfect and changes with time. This imperfection and its evolution creates a thermal contact resistance that reduces the heat transfer and the solidification rate. The resistance to heat flow at the metal–mold interface has a marked influence on the solidification rate of metal castings. A fast cooling rate promotes a fine grained structure in the casting and improves the mechanical properties of the solidified metal [1]. Therefore, an accurate estimation of thermal contact resistance is of practical importance in the casting of metal in a metal mold. This work is an attempt to detect this thermal contact resistance and characterize its evolution with time. We try to analyze and to model heat flow at the metal–mold interface during metal solidification.

Numerous studies of thermal contact resistance were focused on solid–solid metals such as steels, alloys and their environments, for example, air, other gases, or fluids. A general review of thermal contact was provided by [2, 3]. Based on their reviews, thermal contact resistance studies of several fields have been explored, such as porous materials, composite materials, layered materials, microelectronics, and biomedicine.

To date, there are few studies published regarding thermal resistance contact during metal casting and no known correlation is available for the prediction of interface heat transfer coefficient between the mold and casting surfaces from fundamental principles. There is a general review on the subject in Viskanta [4].

Prates et al. [5] have proposed a mechanism to explain the initial formation of metal–mold interface with solid–solid contact based on their work with aluminum alloys. The postulating is based on the fact that, on microscopic scale, the surface of a permanent mold is not completely smooth and consists of small asperities production from the surface profile. When liquid metal first approaches the mold surface, contact occurs at the peaks of asperities. Rapid cooling at these peaks causes solidification of the liquid metal to nucleate from these sites. At the same time, the surface tension of liquid metal and subsequent rapid growth of solidification from the nucleation sites prevents the solidifying metal from wetting the valleys on the surface profile of the mold.

Ho et al. [6, 7] have shown that it is possible, with the formation of an interfacial gap, to calculate the interfacial heat transfer coefficient by a simple superposition of gas conduction and radiation via the quasi-steady state approximation. But the question is how to determine precisely the gap thickness. Pehkle [8] has done several simulations of solidification of various castings in different type of molds and has noted the difficulties of lack of proper material property data. He has also realized the importance of mold–metal interface in solidification process.

Srinivasan et al. [9] have observed that it is possible to get useful numerical solutions for temperature distribution in solidifying castings only if the interface heat transfer coefficients are known with sufficient accuracy. Erickson [10] has noted that in spite of the advances made in the numerical methods developed for handling solidification problems, the simulation results are very much hampered by the lack of availability of material properties near solidification temperatures and lack of reliable data on heat transfer coefficients at the interface. All these authors expressed the considerable lack in the heat interface coefficient area. Isaac et al. [11, 12] have studied the formation and distribution of air gap during the solidification of castings in metallic molds. They have concluded that the value of heat transfer coefficient at the interface is not constant, but varies with time. It decreases as the solidification of aluminum casting in metallic mold proceeds. The value of heat transfer coefficient also changes from point to point on the surface of casting. This being maximum at the middle of the casting surface. The time of start of air gap formation at the corner is less than at the middle. As coating thickness increases, there is an increase in the time of start of air gap formation both at the corner and at the middle of the metallic mold.

Danes et al. [13] have studied the influence of the capillary gas traps during the metal solidification on a level wall. This study is centered on the capillary trapping at ambient atmosphere. The insulate coating at the liquid–solid interface is discontinuous gaseous. With a specific contact fashion between liquid and solid and a regular two-dimension surface roughness kind, they have studied the influence of, the wall roughness surface, the superficial tension of liquid and the contact angle between gas–liquid–solid. They show that the solidification starts at the gas–liquid–solid contact point. In the beginning the phase change boundary is inclined and becomes horizontal later. Thermal contact resistance increases when the surface curvature and the solidification speed increase. When the volume of the metal is not simply convex but limited by an inner and an external wall, if the solidification starts from the inner wall and finishes on the external wall, thermal contact resistance is greater than in the opposite case where solidification starts from the external wall and finishes on the inner wall. Thermal contact resistance is more sensitive, in the metal solidification case, to the temperature variation than of the contact case between two solid metals.

All the previous studies show the importance of the appearance and the evolution of thermal contact resistance on the solidification process. The first instance of this process, which seem to be determinant in the ulterior evolution of the thermal contact condition, are not very studied. To have more information on the real contact conditions, in the first stages of the solidification process ($t \geqslant 1$ ms), we have developed this study.

The establishment of the thermal contact resistance, in the first instants of contact, is closely related to the time of the constriction establishment. In ref. [14], we have shown in detail that the constriction phenomenon can be considered well established for $t \geqslant 1$ ms. We have shown also that the establishment time is related to thermophysical properties of the mold and casting and the size of an elementary contact area. Then, in this work where experiment data are available for $t \geqslant 1$ ms, the classical scheme of thermal contact resistance can be used.

2. Principle of experiment and estimation

To simulate casting operation, a specific casting experiment has been developed for the heat transfer study across the metal–mold interface. This experiment consists in the falling of molten metal drop on a cooled substrate. The geometric configuration is shown in Fig. 1. Using this specific experiment, the initial contact time and the two initial temperatures of casting and mold are perfectly well known. This experiment can be easily used to analyze the effect of many factors such as substrate surface roughness, substrate coating, ...

The non-perfect thermal contact between the casting and the substrate surface is quantified by estimating continually the heat flux and the temperatures on the left and the right of the drop-substrate interface. Then if $T_c(a,t)$ is the bottom casting surface temperature and $T_s(a,t)$ is the substrate surface temperature (mold), thermal contact resistance across the interface can be expressed as:

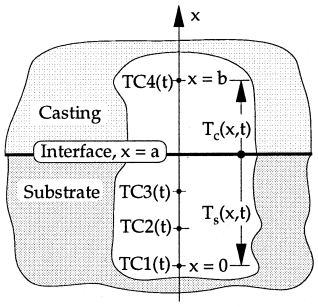

Fig. 1. Geometric configuration.

$$\mathscr{R}(t) = \frac{T_c(a,t) - T_s(a,t)}{\varphi_{int}(t)} \tag{1}$$

where $\varphi_{int}(t)$ is heat flux density through the interface.

In a first step, the incoming heat flux through the substrate $\varphi_{int}(t)$ and the substrate surface $T_s(a,t)$ are estimated by solving inverse heat conduction problem in the substrate region. This procedure uses measured temperatures inside the substrate as additional information. The position of sensors close to the substrate surface is essential and conditions the temporal resolution limit of the experiment. Once the heat flux at the interface is estimated, in a second step, the surface temperature in the casting side is estimated by solving the direct heat conduction problem with phase change in casting region. A measured temperature in casting region and the estimated heat flux are used as boundary conditions. To get temperature measurement in the casting region during the drop fall, a thermocouple is stretched in ambient near the substrate surface. At the end of the falling process, this sensor finds itself drowned in solidifying metal.

2.1. Substrate surface temperature and heat flux estimation

The inverse problem of interest consists in determining the heat flux or the temperature at the active surface of the substrate, ($x = a$) see Fig. 1, from temperature measurements at fixed locations inside the substrate. For the non-linear case, the unknown functions $T_s(a,t)$ and $\varphi_{int}(t)$ need to be determined from the following mathematical formulation of the direct problem in the substrate region

$$\rho_s Cp_s(T)\frac{\partial T_s(x,t)}{\partial t} = \frac{\partial}{\partial x}\left(\lambda_s(T)\frac{\partial T_s(x,t)}{\partial x}\right), \quad 0 < x < a, \quad 0 < t < t_f \tag{2}$$

$$T_s(0,t) = T_0(t), \quad 0 < t \leqslant t_f \tag{3}$$

$$\alpha_1 T_s(a,t) - \alpha_2 \lambda_s(T)\frac{\partial T_s(a,t)}{\partial x} = U(t), \quad 0 < t \leqslant t_f \tag{4}$$

$$T_s(x,0) = F(x), \quad 0 \leqslant x \leqslant a \tag{5}$$

with $(\alpha_1 = 1, \alpha_2 = 0)$ when estimating $T_s(a,t)$ and $(\alpha_1 = 0, \alpha_2 = 1)$ when estimating the heat flux at the interface $\varphi_{int}(t)$. The boundary condition $T_0(t)$ is the temperature history measured by the sensor $TC_1(t)$. As additional information temperature histories

$$f_i(t), \quad i = 1, \ldots, N \tag{6}$$

measured by N sensors installed inside the substrate are used.

The solution of the boundary problem, equations (2)–(5) with the temperature or the heat flux unknown can be obtained from the condition of minimizing the mean-square deviation:

$$J(U) = \sum_{i=1}^{N} \int_0^{t_f} [T_s(x_i, t; U) - f_i(t)]^2 \, dx \quad (7)$$

where $T_s(x_i, t; U)$, $f_i(t)$ represent the estimated and measured temperature at different points in the substrate corresponding to the thermocouple locations. The inverse problem is reduced to minimize the residual functional (7) under constraints given by the boundary value problem (2)–(5). Following [15, 16], we use a parametric representation of the function to be estimated in the form

$$U(t) = \sum_{i=1}^{M} u_i \varphi_i^k(t) \quad (8)$$

where u_i are unknown coefficients. In our case, the chosen basis functions $\varphi_i^k(t)$ are B-spline functions of order $k = 4$ (cubic spline). The ref. [17] gives more details on the properties and the use of the B-spline functions. The estimation of the function $U(t)$ is reduced to determine a set of parameters u_i represented by the vector

$$\mathbf{U}^T = [u_1, u_2, \ldots, u_M]^T. \quad (9)$$

In this case, the residual functional is reduced to a function of M variables.

2.1.1. Minimization procedure

The residual functional minimization with respect to desired parameters is the most important procedure in algorithms for solving inverse problems. To do that, we use the conjugate gradient method [15, 18]. The successive improvements of desired parameters are built as

$$\boldsymbol{U}^{s+1} = \boldsymbol{U}^s + \gamma^s \boldsymbol{D}^s, \quad s = 1, \ldots, s^* \quad (10)$$

where s is the iteration number, s^* is the last iteration number, γ^s is the descent parameter, $\boldsymbol{U}^s$ is the unknown vector to be estimated, $\mathbf{U} = [u_1, u_2, \ldots, u_M]^T$, $\boldsymbol{D}^s$ is the descent direction vector, $\boldsymbol{D} = [d_1, d_2, \ldots, d_M]^T$.

The vector of the descent direction is given by:

$$\boldsymbol{D}^s = -\nabla \boldsymbol{J}^s + \beta^s \boldsymbol{D}^{s-1} \quad (11)$$

where

$$\beta^s = \frac{\langle \nabla \boldsymbol{J}^s - \nabla \boldsymbol{J}^{s-1}, \nabla \boldsymbol{J}^s \rangle}{(\nabla \boldsymbol{J}^s)^2}, \quad \beta^0 = 0 \quad (12)$$

where $\langle , \rangle$ is the scalar product. With the parameterization form, the gradient of the residual functional (7) is given by the vector

$$\nabla \boldsymbol{J} = [\nabla J_1, \nabla J_2, \ldots, \nabla J_M]^T. \quad (13)$$

In considering the substrate region as N layers with perfect thermal contact between them, see refs. [15, 19], it can be shown that the jth component of the vector $\nabla \boldsymbol{J}$ has the following analytical expression

$$\nabla J_j = \int_0^{t_f} \left(\alpha_2 \psi_s^N(a, t) + \alpha_1 \lambda_s(T) \frac{\partial \psi_s^N(a, t)}{\partial x} \right) \varphi_j^k(t) \, dt, \quad j = 1, \ldots, M \quad (14)$$

where $\psi_s^i(x, t)$ is a solution of the following adjoint problem:

$$-\rho_s C p_s(T) \frac{\partial \psi_s^i(x, t)}{\partial t} = \lambda_s(T) \frac{\partial^2 \psi_s^i(x, t)}{\partial x^2} \quad i = 1, \ldots, N, \quad x_i < x < x_{i+1}, \quad 0 < t \leqslant t_f \quad (15)$$

$$\psi_s^i(x, t_f) = 0, \quad x_i < x < x_{i+1}, \quad i = 1, \ldots, N \quad (16)$$

$$\psi_s^1(0, t) = 0, \quad 0 < t \leqslant t_f \quad (17)$$

$$\psi_s^i(x_{i+1}, t) = \psi_s^{i+1}(x_{i+1}, t), \quad i = 1, \ldots, N-1, \quad 0 < t \leqslant t_f \quad (18)$$

$$\lambda_s(T) \left(\frac{\partial \psi_s^{i+1}(x_{i+1}, t)}{\partial x} - \frac{\partial \psi_s^i(x_{i+1}, t)}{\partial x} \right) = 2[T_s^i(x_{i+1}, t) - f_i(t)] \quad i = 1, \ldots, N-1, \quad 0 < t \leqslant t_f \quad (19)$$

$$\alpha_1 \psi_s^N(a, t) + \alpha_2 \lambda_s(T) \frac{\partial \psi_s^N(a, t)}{\partial x} = 0, \quad 0 < t \leqslant t_f. \quad (20)$$

To estimate γ^s, a linear approximation is used [15]:

$$\gamma^s = -\frac{\sum_{i=1}^{N} \int_0^{t_f} [T_s^i(x_i, t) - f_i(t)] \Delta T_s^i(x_i, t) \, dt}{\sum_{i=1}^{N} \int_0^{t} [\Delta T_s^i(x_i, t)]^2 \, dt} \quad (21)$$

where $\Delta T_s^i(x_i, t)$ is the solution of the following boundary value-problem in variations

$$\rho_s \frac{\partial [C p_s(T) \Delta T_s^i(x, t)]}{\partial t} = \frac{\partial^2 [\lambda_s(T) \Delta T_s^i(x, t)]}{\partial x^2} \quad i = 1, \ldots, N, \quad x_i < x < x_{i+1}, \quad 0 < t \leqslant t_f \quad (22)$$

$$\Delta T_s^i(x, 0) = 0, \quad 0 \leqslant x \leqslant a, \quad i = 1, \ldots, N \quad (23)$$

$$\Delta T_s^1(0, t) = 0, \quad 0 < t \leqslant t_f \quad (24)$$

$$\Delta T_s^i(x_{i+1}, t) = \Delta T_s^{i+1}(x_{i+1}, t), \quad i = 1, \ldots, N-1, \quad 0 < t \leqslant t_f \quad (25)$$

$$\frac{\Delta T_s^i(x_{i+1}, t)}{\partial x} = \frac{\Delta T_s^{i+1}(x_{i+1}, t)}{\partial x}, \quad i = 1, \ldots, N-1, \quad 0 < t \leqslant t_f \quad (26)$$

$$\alpha_1 \Delta T_s^N(a, t) - \alpha_2 \lambda_s(T) \frac{\partial \Delta T_s^N(a, t)}{\partial x} = \Delta U(t), \quad 0 < t \leqslant t_f. \quad (27)$$

The three different problems are solved numerically using control volume method [20]. When all unknowns used in the iterative procedure, formula (10), are defined, we can now solve the inverse problem using additional information i.e. measurements. The measurements are always noised and their use may give unstable solutions. In fact these kind of problems are known to be ill-posed. On the other hand, their solution does not satisfy the general requirement of existence, uniqueness and stability under

small changes in the input data. To stabilize the inverse problem solution, there are different regularizing methods [15, 21, 22]. The iterative regularization method is used in our case to solve inverse heat conduction problems.

2.1.2. Iterative regularization method

The main idea of the iterative regularization method, [15, 16], consists in finding a solution of the initial problem (7) such

$$J^{s*} \simeq \delta^2 = \sum_{i=1}^{N} \int_0^{t_f} \sigma_i^2 \, dt \tag{28}$$

where $s*$ is the number of the last iteration (regularization parameter), δ^2 is a time integrated measurement error and σ_i is the standard deviation for each sensor. We observe that the regularization criterion is directly related to the measurement error. The main difficulty of this method is the unknown δ^2. To estimate δ^2, we have chosen the smoothing technique.

2.1.3. Smoothing of measured temperature

In our case we want to smooth a measured temperature $f(t_i)$ by a smooth function $f^*(t_i)$ in the sense of least square. We use the B-splines function of order $k = 4$. The smoothed function is written as

$$f^*(t_i) = \sum_{j=1}^{P} c_j \varphi_j^k(t_i) \tag{29}$$

where $\varphi_i^k(t), i = 1, \ldots, P$ are known basis functions. If the smoothing function $f^*(t_i)$ is obtained, the integrated error can be computed as

$$\delta^2 = \int_0^{t_f} [f^*(t) - f(t)]^2 \, dt = \int_0^{t_f} \left[\sum_{j=1}^{p} c_j \varphi_j^k(t) - f(t) \right]^2 dt \tag{30}$$

where P is the number of parameters c_i. The problem of smoothing is reduced to estimate the c_j coefficients.

The choice of the optimum number of parameters or basis functions P^* is not a simple question. For the moment we choose it by using visual approach. Indeed, we start with a small number of parameters and then we add one by one until the smooth profile becomes unstable. When we observe that the smoothed curve is in agreement with the physical evolution of the profile and when it becomes unstable we stop increasing the number of parameters and we choose the last one as optimal.

2.1.4. Numerical simulations of smoothing

Several numerical experiments were carried out to test the computational procedure for estimating an evolution of the thermal contact resistance. The first stage was to simulate the smoothing of measured temperature histories and check the accuracy of estimating the generalized measurement error δ^2.

To test the elaborated smoothing technics, we try to rebuild a noised temperature profile which we know the δ_{ex}^2 and the exact profile. To the initial temperature curve we add a white and normal noise. The perturbation is defined as $B = \omega T_{max} \Delta_{max}$ where ω is random number generator $[-1, +1]$, T_{max} is the maximum temperature value in the profile and Δ_{max} is the magnitude of the perturbation (in %). Our simulations are conducted using $N = 1001$ measurement points, $P = 101$ number of parameters, $k = 4$ order of B-splines and $\Delta_{max} = 2\%$. We have smoothed the noised data. The result of smoothing is shown in Fig. 2. The smoothed profile is obtained with an error of 1.17% and the error of the computed δ^2 is less than 1.2%.

The evolution of the residual between noised and smoothed temperature and exact and smoothed temperature is plotted in Fig. 3. We observe that the error of estimated function is still small in comparison with the evolution of the added noise. This result shows that this approach can be used to smooth real noised data.

2.1.5. Simulation of surface temperature and heat flux estimation

The second stage was to verify the algorithm for solving the inverse problem. In Fig. 4, we have simulated the substrate surface temperature with and without regularization. This estimation procedure uses the parametrized form of the unknown function to be estimated and the computed δ^2 as stopping criteria, formula (28). With the use of parametrized functions to approximate the unknown surface evolution, it is possible to stabilize a solution of the inverse problem by reducing the number of approximation parameters P in comparison with the number of time steps in finite difference grid N. That gives the stabilization in the sense of least squares. But doing so, a large enough number P should be used to obtain a good approximation accuracy. In our case, the ratio N/P was about 10. One can see in Fig. 4 that this ratio is not sufficient to obtain a stable solution of the inverse problem. A stable solution was estimated with the residual criterion (28). In Fig. 4, we can observe that the residual becomes large at the end (at time > 0.9 s). This difference is caused by the end condition given in the adjoint problem [equation (16)]. Since the adjoint variable $\psi_s(x, t)$ is always equal to zero at t_f, there is no evolution in the iterative procedure when estimating the unknown $U(t)$.

2.2. Casting surface temperature estimation

For obtaining the casting temperature profile during the solidification, it is necessary to solve the heat conduction problem with phase change in the casting region. With the heat flux $\varphi_{int}(t)$ at the interface known, the temperature field in the casting region can be computed using the estimated heat flux and the measured tem-

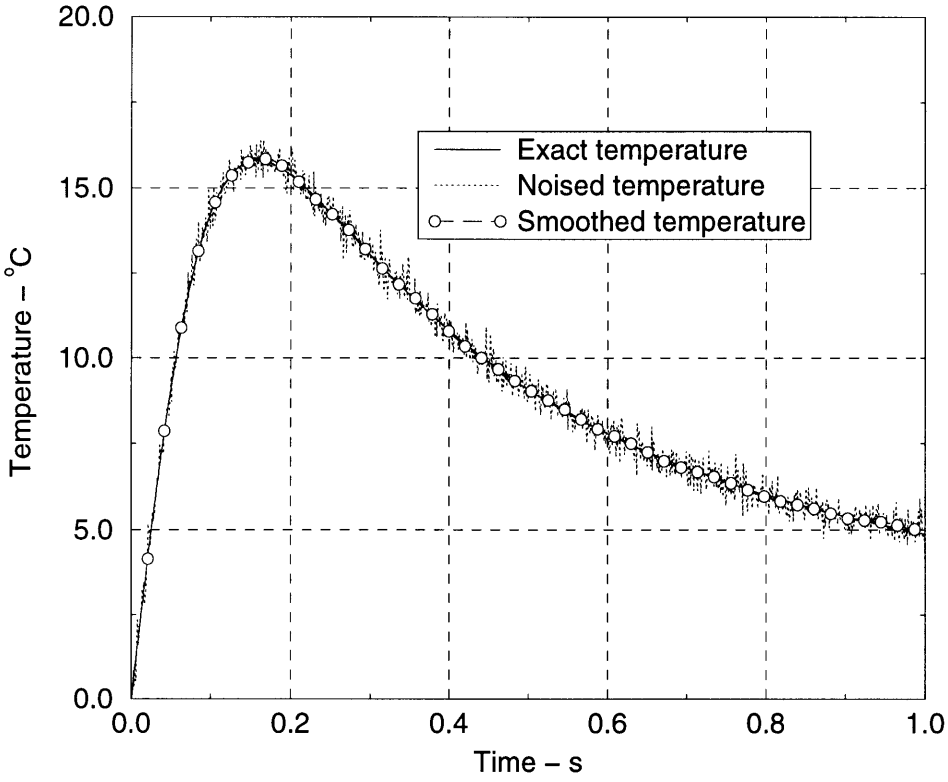

Fig. 2. Rebuilt noised data.

perature given by thermocouple $TC_4(t)$ as the boundary conditions. The numerical procedure is based on the enthalpy method (fixed grid domain) [23, 24]. The mathematical formulation of this problem is given by

$$\rho_c \frac{\partial H_c(T)}{\partial t} = \frac{\partial}{\partial x}\left(\lambda_c(T)\frac{\partial T_c(x,t)}{\partial x}\right), \quad a < x < b, \quad 0 < t \leqslant t_f \tag{31}$$

$$-\lambda_c(T)\frac{\partial T_c(a,t)}{\partial x} = \varphi_{int}(t), \quad 0 < t \leqslant t_f \tag{32}$$

$$T_c(b,t) = T_b(t), \quad 0 < t \leqslant t_f \tag{33}$$

$$T_c(x,0) = T_c^i, \quad a \leqslant x \leqslant b \tag{34}$$

$\varphi_{int}(t)$ is the heat flux received by the substrate and $T_b(t)$ is the temperature measured by the sensor $TC_4(t)$. The enthalpy is related to the temperature via:

$$H_c(T) = \int_{T_0}^{T} Cp_c(\theta)\,d\theta, \quad T < T_m$$

$$\int_{T_0}^{T} Cp_c(\theta)\,d\theta \leqslant H_c(T) \leqslant \int_{T_0}^{T} Cp_c(\theta)\,d\theta + L_c, \quad T = T_m$$

$$H_c(T) = \int_{T_0}^{T} Cp_c(\theta)\,d\theta + L_c, \quad T > T_m \tag{35}$$

T_0 is a fixed temperature less than T_m. From the above formula (35), one can observe a big non-linearity of the enthalpy as function of temperature at the melting temperature T_m. Due to the heat jump at the phase change boundary, usual numerical methods used to solve such problems cannot overcome this non-linearity. Several authors [23, 24] have tried to linearize the jump in the enthalpy at the melting temperature.

In our case we have chosen apparent heat capacity model to solve the phase problem in the casting region. The left member of equation (31) can be written as

$$\rho_c \frac{\partial H_c(T)}{\partial t} = \rho_c \frac{\partial H_c(T)}{\partial T}\frac{\partial T_c(x,t)}{\partial t} = \rho_c Cp_a(T)\frac{\partial T_c(x,t)}{\partial t} \tag{36}$$

where $Cp_a(T)$ is an apparent heat capacity of casting. The derivative of $H_c(T)$ with respect to temperature is infinite at melting temperature point T_m. To linearize this jump, we approximate $Cp_a(T)$ by polynomial function of degrees 5, in a small temperature interval, ΔT, around

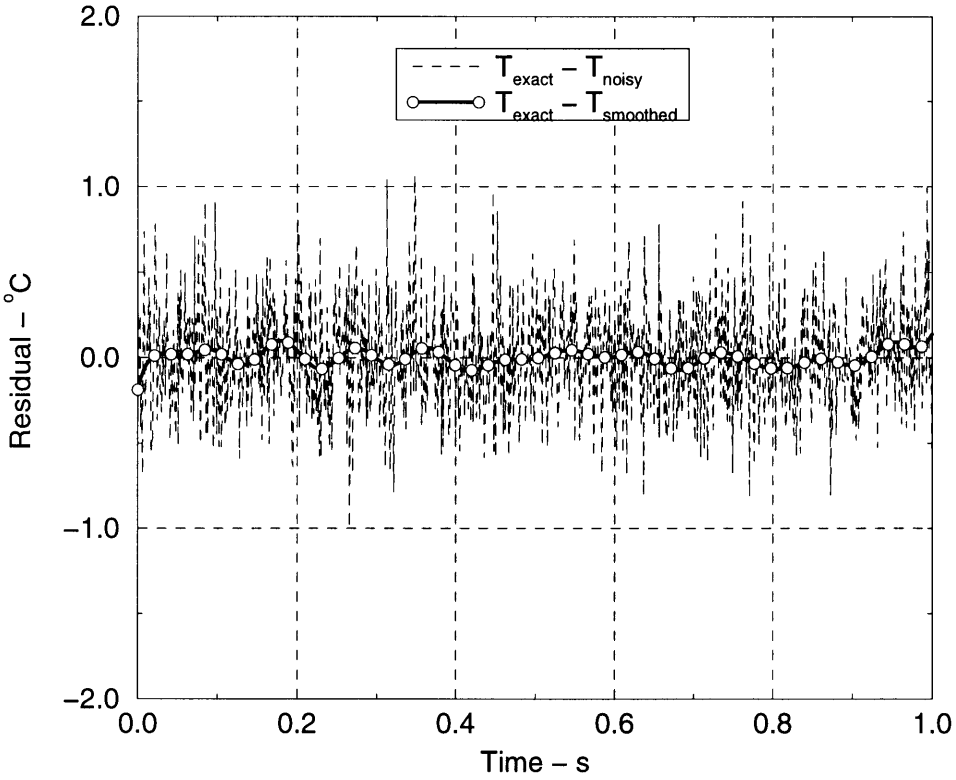

Fig. 3. Comparison between residues.

the phase change point. To simulate the temperature jump, the maximum of the polynomial function must occur at T_m. This approximation is written as

$$Cp_a(T) = A_0 + A_1 T + A_2 T^2 + A_3 T^3 + A_4 T^4 + A_5 T^5 \tag{37}$$

with the following conditions

$$Cp_a(T_1) = Cp_s(T_1)$$

$$Cp_a(T_2) = Cp_l(T_2)$$

$$\frac{dCP_a(T)}{dT} = \frac{dCp_s(T)}{dT}, \quad T = T_1$$

$$\frac{dCp_a(T)}{dT} = \frac{dCp_l(T)}{dT}, \quad T = T_2$$

$$\frac{dCp_a(T)}{dT} = 0, \quad T = T_m$$

$$\int_{T_1}^{T_m} Cp_s(\theta)\,d\theta + \int_{T_m}^{T_2} Cp_l(\theta)\,d\theta + L_c = \int_{T_1}^{T_2} Cp_c(\theta)\,d\theta \tag{38}$$

where T_1 and T_2 are given, respectively, by $T_1 = T_m - \Delta T/2$ and $T_2 = T_m + \Delta T/2$. $CP_s(T)$ and $Cp_l(T)$ represent the heat capacity of solidified and liquid metal in casting region. The two first conditions show the connection of the apparent heat capacities $Cp_a(T)$ with the solid phase $Cp_s(T)$ and the liquid phase $Cp_l(t)$ heat capacity of casting. The six conditions given in formula (38) allow the estimation of the A_i coefficients used in the approximation model, equation (37).

To validate this method, the one-dimensional freezing problem defined in [25] will be used as the test problem. Thermophysical properties of material and the thermal conditions considered were

$$\rho_s = \rho_l = 1\ \text{kg m}^{-3}, \quad \lambda_s = \lambda_l = 2\ \text{W m}^{-1}\ \text{K}^{-1}$$

$$Cp_s = Cp_l = 2.5\ \text{MJ kg}^{-1}\ ^\circ\text{C}^{-1}, \quad L_c = 100\ \text{MJ kg}^{-1}$$

$$T_m = 0, \quad T(x,0) = 7^\circ\text{C}, \quad T(0,t) = -7^\circ\text{C}$$

$$T(x,L) = 7^\circ\text{C}, \quad \Delta T = 2^\circ\text{C}, \quad L = 1\ \text{m}.$$

The result of the simulation is shown in Fig. 5. The maximum difference between computed and analytical solution is less than 1.2°C. The error of computed temperature is about 0.42%. This result allows us to use such a method in our estimation.

3. Conclusion

From the above work, it can be summarized that the principle of a specific experiment and numerical algorithm

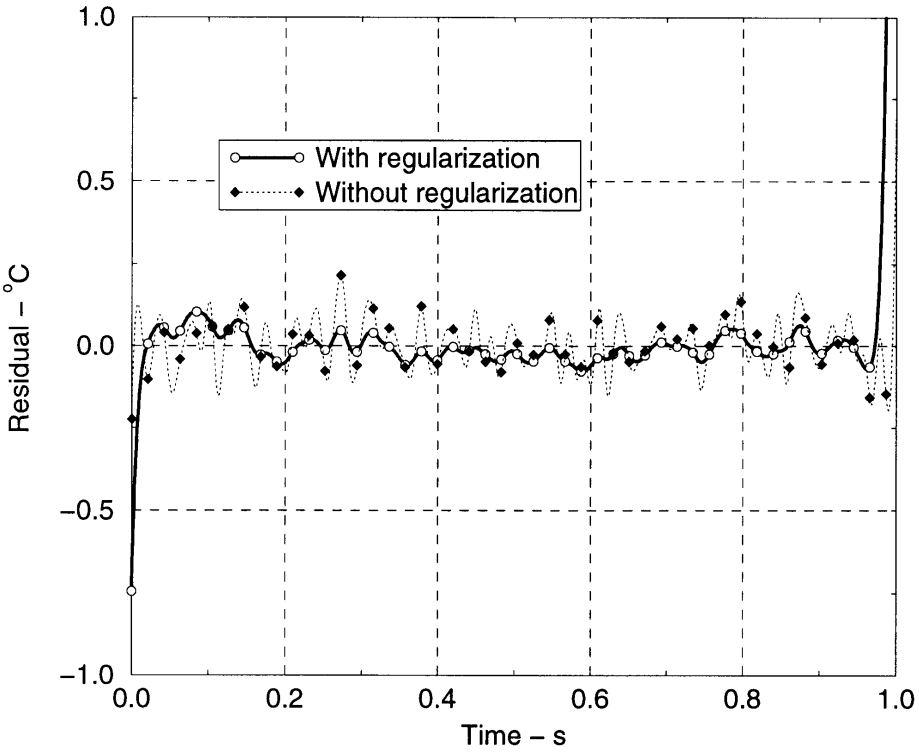

Fig. 4. Regularization effect on the stabilization of the solution.

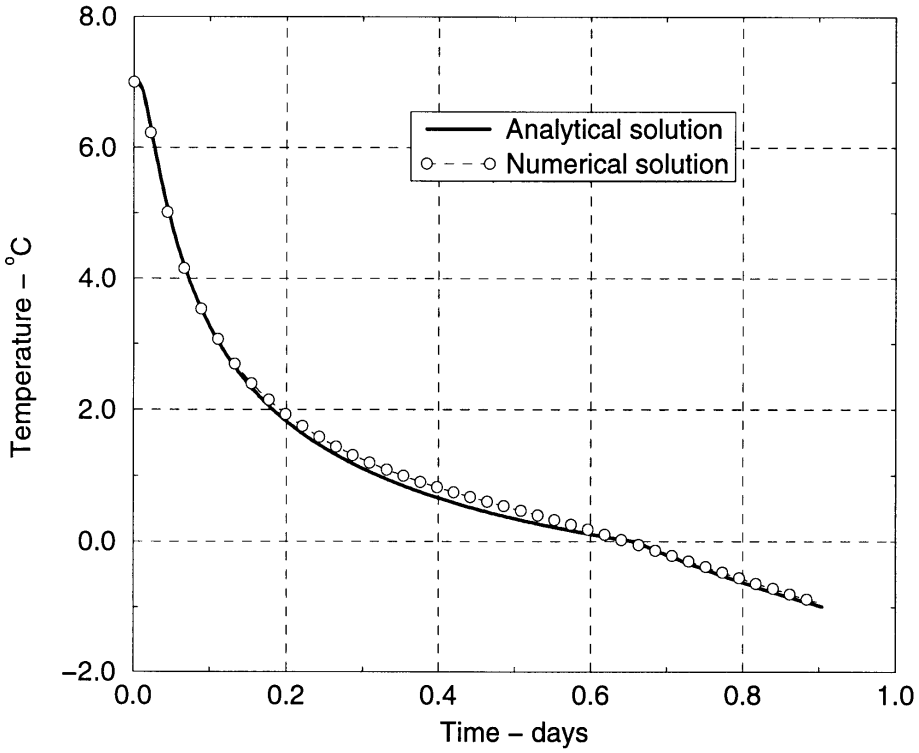

Fig. 5. Simulation of solidification in half space.

were developed to estimate the thermal contact conditions, as a time function, during the early stages of solidification during continuous casting. The drop-substrate experiment created to simulate experimentally the casting conditions allows us to analyze the phenomenon of the establishment and evolution of the thermal contact resistance during the initial period of contact.

First obtained results show good enough efficiency of the developed computational tools. A numerical procedure is built to estimate the heat flux at the interface and the two surface temperatures of casting and substrate. To obtain heat flux and the substrate surface temperature, the inverse heat conduction problem is solved in the substrate region. To stabilize the solution of the inverse problem, we have smoothed the temperature measurements. Numerical simulations have shown that we can get δ^2 with 5% error. We have shown that the use of parametrization is not sufficient to stabilize solution. Its use without any regularization criteria leads to unstable solutions.

The tools developed here can be used to set up an accurate experiment and to study the thermal contact resistance at the interface between solidifying metal and the mold. The influence of different factors such as temperature, casting duration, lubrication type, surface roughness, thermal conductivity of material mold and metal casting, pressure, wetting of the mold wall and other factors will be analyzed in the next paper. All these factors are going to increase the complexity of thermal contact resistance in metal casting.

References

[1] W. Kurz, D.J. Fisher, Fundamentals of Solidification, Trans. Tech Publications, Lausanne, 1989.

[2] J.P. Bardon, Heat transfer at solid–solid interface, basic phenomenons, recent works, In: Fourth Eurotherm, vol. 1, Nancy, France, September 1988, pp. 40–74.

[3] L.S. Fletcher, Recent developments in contact conductance heat transfer, A.S.M.E. J. Heat Transfer 110 (1988) 1059–1070.

[4] R. Viskanta, Heat transfer during melting and solidification, A.S.M.E. J. Heat Transfer 110 (1988) 1205–1219.

[5] M. Prates, H. Biloni, Variables affecting the nature of the chill zone, Metall. Trans. 3 (1972) 1501–1510.

[6] K. Ho, R.D. Pehlke, Mechanisms of heat transfer at a metal–mold interface. AFS Transactions 92 (1984) 587–598.

[7] K. Ho, R.E. Pehlke, Metal–mold interfacial heat transfer, Metall. Transaction 16B (1985) 585–596.

[8] R.D. Pehlke, The interface in computer simulation of heat transfer in metallurgical processes, Metallurgical Engineer Quarterly 3 (1971) 9–13.

[9] M.N. Srinivasan, Heat transfer coefficients at casting mold interface during solidification of flake-graphite cast iron in metallic molds, Indian Journal of Technology 20 (1971) 12.

[10] W.C. Erickson, Computer simulation of solidification, AFS Cast Metals Research Journal 5 (1980) 30.

[11] G.R. Reddy, J. Issac, G.K. Sharma, Variation of heat transfer coefficient during solidification of casting in metallic molds, The British Foundryman II (1985) 465–468.

[12] J. Issac, G.R. Reddy, G.K. Sharma, Experimental investigation of the influence of casting parameters on the formation and distribution of air-gap during the solidification of castings in metallic molds, AFS Transactions 93 (1985) 29–34.

[13] F.E. Danes, J.P. Bardon, Résistance de contact lors de la solidification: rôles des pièges à gaz, Journée S.F.T., Paris, 1991.

[14] T. Loulou, Heat transfer modelling at the mold-casting interface during the solidification process, Ph.D. thesis, University of Nantes, Nantes, France, 1995.

[15] O.M. Alifanov, E.E. Artyukhin, S.V. Rumyantsev, Extreme Methods of Solving Ill-Posed Problems and their Applications to Inverse Heat Transfer Problems, Begell House, New York, 1995.

[16] O.M. Alifanov, Inverse Heat Transfer Problems, Springer-Verlag, Berlin, 1994.

[17] C. de Boor, A Practical Guide to Splines, 1st ed., Springer-Verlag, Berlin, 1981.

[18] Y. Jarny, M.N. Ozişik, J.P. Bardon, A general optimization method using adjoint equation for solving multidimensional inverse heat conduction, Int. J. Heat Mass Transfer 34 (11) (1991) 2911–2919.

[19] M.N. Ozişik, Boundary Value Problem of Heat Conduction, Dover, New York, 1989.

[20] S.V. Patankar, Numerical Heat Transfer and Fluid Flow, McGraw-Hill, New York, 1980.

[21] A.N. Tikhonov, V.Y. Arsenin, Solution of Ill-posed Problems, Winston and Sons, Washington D.C., 1977.

[22] V.A. Morozov, Methods for Solving Incorrectly Posed Problems, Springer-Verlag, Berlin, 1984.

[23] J. Crank, Free and Moving Boundary Problems, Oxford University Press, London, 1984.

[24] V. Alexiades, A.D. Solomon, Mathematical Modeling of Melting and Freezing Processes, 1st ed., Hemisphere, Washington, 1993.

[25] V.R. Voller, M. Cross, Accurate solution of moving boundary problems using the enthalpy method, Int. J. Mass Transfer 24 (1981) 545–556.